LCC-0126
SLAC-TN-03-051
September 2003

Linear Collider Collaboration Tech Notes

Single Bunch Electron Cloud Effects in the NLC Beam Delivery System

David Chen, Arthur Chang, M. T. F. Pivi, T. O. Raubenheimer

Stanford Linear Accelerator Center
Stanford University
Stanford, CA

Abstract: A positron beam passing through a linear collider beam delivery line is finely focused to desired specifications. Unwanted additional focusing is generated by beam-electron-cloud interactions that can cause beam size increases at the IP when there are high cloud densities. This paper examines the severity of the electron cloud effects and assesses the critical cloud density.

Single Bunch Electron Cloud Effects in the NLC Beam Delivery System

David Chen, Arthur Chang, Dan Bates, Mauro Pivi, Tor Raubenheimer
Stanford Linear Accelerator Center, Stanford University, Stanford, CA 94309

Abstract

A positron beam passing through a linear collider beam delivery beam line is finely focused to desired specifications during collimation and especially in Final Focusing (FFS). Undesired additional focusing is generated by beam-electron cloud interactions, which typically leads to beam size increases at high cloud densities. This paper examines the severity of the electron cloud effects and assesses the critical cloud density.

1. Introduction

The generation of an electron cloud in the beam delivery system may potentially have unwanted effects on the passing positron beam. In the NLC design, the bunch train is roughly 268 ns in length. Depending on the vacuum chamber radius, material and conditioning, an electron cloud can be generated which may approach the neutralization density. For example, with a 1cm radius chamber and a peak Secondary Electron Yield (SEY) of 2, the electron cloud reaches a density of roughly 1e14 e/m^3 by the end of the positron bunch train.

If the cloud density is allowed to grow to high densities along the bunch train, various effects may appear in the FFS. In this note, we study single bunch effects that impact the spot size at the IP. The relative significance of these effects was assessed with simulations using CLOUD_MAD, a program that tracks the beam behavior in the presence of an electron cloud given a range of physical parameters. Changes in the beam were indicated by variations in the beam emittances and spot sizes near the IP. Unless otherwise stated, all data are normalized to emittances and spot sizes at 1e7 e/m^3, where the electron cloud has no observable effect.

A significant, near-exponential growth in emittances and spot sizes occurred above what we now designate a threshold cloud density (~1e11 e/m^3). Below this, the beam shows little variation; beyond this, the beam grows rapidly. In the following, we describe the setup of the simulation code CLOUD_MAD and the series of studies that were performed. We estimate the importance of two of the possible effects: first, phase advance changes through the Chromatic Correction Section (CCS) due to focusing from the beam-electron interaction that may impact the compensation of the

geometric aberrations and, second, the direct spot size change at the IP due to the additional focusing. We study beams with both a correlated and an uncorrelated incoming energy spread which in this case has an impact similar to that described in Ref. [1].

2. Stabilization of Simulation Parameters

The application CLOUD_MAD approximates the actual BDS environment by reading input parameters, such as initial cloud density, bunch charges, sampling grid sizes, and energy correlation. Meanwhile, it also considers all of the magnet specifications and the design beta functions, reading an Extended File Format (XTFF) file that represents the lattice. For a guide to running CLOUD_MAD, see Bates [2].

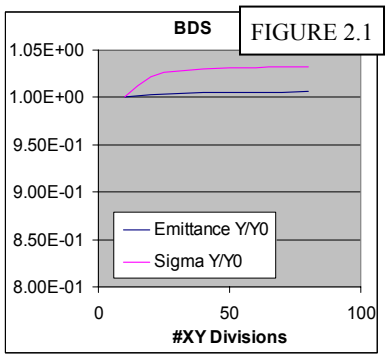

FIGURE 2.1

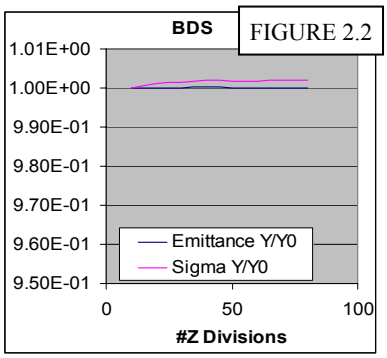

FIGURE 2.2

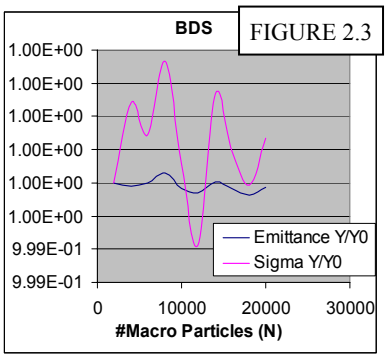

FIGURE 2.3

Before running the tests, several key parameters had to be optimized. Systematic variation in the number of divisions in X, Y, and Z on the grid; the number of macro particles to track; and the cloud boundary radius yielded optimal values for each parameter. The optimal value for X and Y was 60, as the error between 60 and higher numbers of divisions is negligible. See Figure 2.1. Optimization in the number of Z divisions and the number of macro particles to track resulted in 40 and 10,000, respectively. See Figures 2.2 and 2.3.

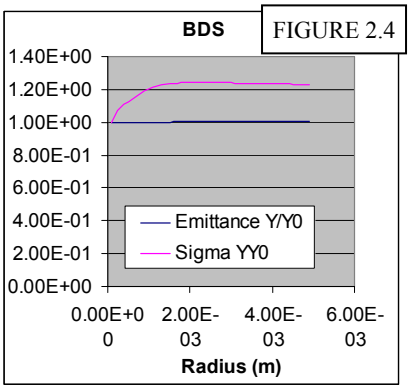

FIGURE 2.4

The cloud boundary radius is the distance beyond which electrons would not be noticeably affected by the passing positron bunches. Let x represent the transverse electron position from the center of the beam and assume a uniform bunch of length L and charge eN. By Gauss' Law, for a cylindrical surface of radius x and length L, the electric field is $E = eN / (2\pi L \varepsilon_0 x) = m_e \ddot{x} / e$. The initial position and velocity of the electron is $x = x_0$ and $v = 0$, respectively. Solving the initial value problem (and assuming non-relativistic mechanics) for the maximum radius at which an electron would reach the center of the bunch at the end of the bunch yields $x_0 \approx \text{sqrt}(4 N r_e L / \pi)$. Thus, for the NLC beam with L=220 μm, we calculate $x_0 = 80\ \mu m$. Since this is smaller than the

transverse beam size, we use a boundary radius of 400 μm in the simulations; larger radii have little effect on either emittance or spot size (see Figure 2.4).

3. Breakdown of the CCS

In terms of changes to the lattice phase advance, we are most concerned with effects in the CCS of the FFS. Energy differences in the beam can either make the focusing waist fall short or surpass the desired location at the IP. The typical solution is to use a pair of sextupoles separated by a $-I$ transformation in spatial coordinates. Several pairs of $-I$ sextupoles are currently implemented for the X and Y planes. If the electrons of the electron cloud change the focusing in this region, they will cause the $-I$ transform to break down, leading to uncompensated nonlinear geometric aberrations. As shown in Figure 3.1, in the presence of sextupoles, an aberration occurs around element 570 that continues for the duration of the FFS. If tune shifts do not constitute a significant effect, however, our concern might be better placed on the direct spot size changes due to the beam-electron focusing effects.

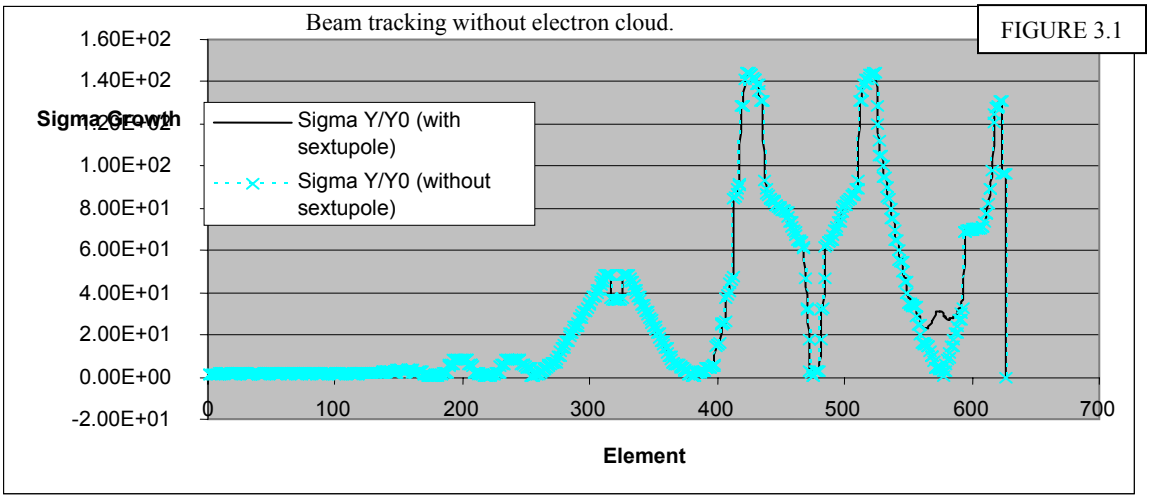

FIGURE 3.1

Changes to the phase advance in the horizontal and vertical directions can be estimated as:

$$\left\{ \begin{aligned} \Delta\nu_x &= \frac{1}{4\pi}\oint \beta_x(s)k_1(s)ds \approx \frac{1}{4\pi}\bar{\beta}_x(s)\bar{k}_1(s)L \\ \Delta\nu_y &= \frac{1}{4\pi}\oint \beta_y(s)k_1(s)ds \approx \frac{1}{4\pi}\bar{\beta}_y(s)\bar{k}_1(s)L \end{aligned} \right\}, \qquad (1)$$

where the electron cloud naturally exerts an electric force on the beam and the normalized focusing gradient is approximately: $k_1 \approx 4\pi n_0 r_e/\gamma$ assuming that the beam and the electron cloud are asymmetric $\sigma_x >> \sigma_y$. In addition, β_x and β_y are the beta functions in X and Y, and L is the length of the beam line. In other words, the phase

advance variation is proportional to both the integrated areas under the respective beta functions (see Figure 3.2) and the electron cloud density (n_0).

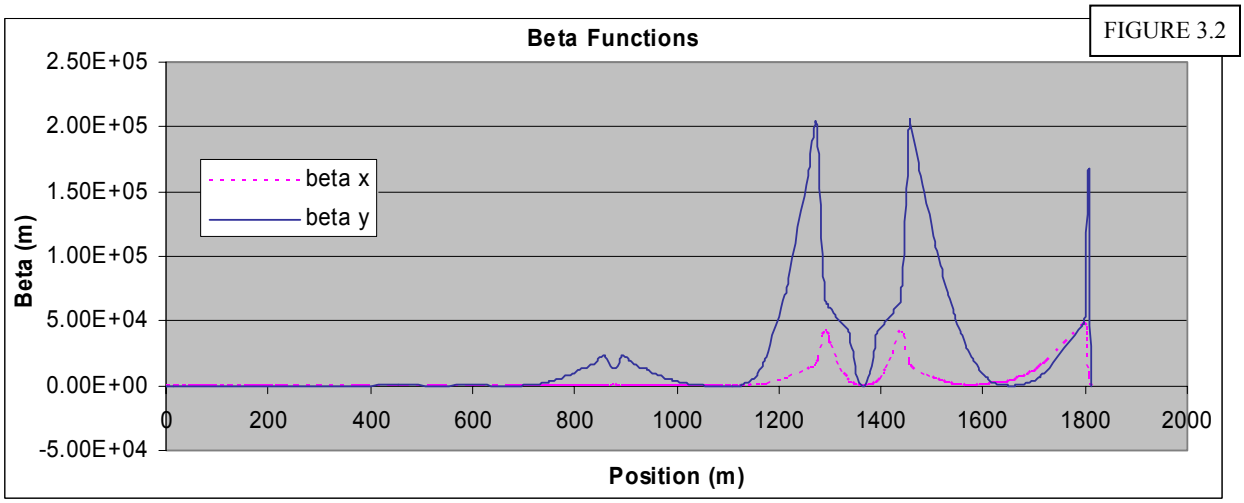

FIGURE 3.2

With an average electron cloud density in the beam of 1e11 e–/m^3 and a beam energy of 250 GeV, the vertical tune shift is 2.5e-2 or 9 degrees in phase. Further assuming that all of the phase shift occurs between the *–I* sextupole pairs, and the geometric aberrations would increase the IP spot size by a factor of 30, the expected $\Delta\sigma/\sigma$ is estimated to be 30%. This needs to be added in quadrature with the spot size, yielding an increase of roughly 15%.

3. Focusing Effects

Direct focusing effects may overshadow the effects of the changes to the phase advance. In both the horizontal and vertical directions, changes to the IP spot size can be estimated as:

$$\left\{ \begin{array}{l} \dfrac{\Delta\sigma_x}{\sigma_x} \approx k_1 \displaystyle\int_0^L \beta_x ds' \sin^2\left[\phi(s)-\phi(s')\right] \\ \dfrac{\Delta\sigma_y}{\sigma_y} \approx k_1 \displaystyle\int_0^L \beta_y ds' \sin^2\left[\phi(s)-\phi(s')\right] \end{array} \right\}, \qquad (2)$$

where $\phi(s)$ is the phase advance and L is again the length of the beam line. As the electron cloud density increases, the focusing increases and this will change the location of the beam waist at the IP. Additionally, since $k_1 \propto n_0 r_e/\gamma$, an order of magnitude increase in the cloud density creates at least an order of magnitude increase in $\Delta\sigma/\sigma$. With a 250 GeV beam and an electron density of 1e11 e–/m^3 inside the beam, the vertical IP spot size $\Delta\sigma/\sigma$ is estimated to be 30%, very similar to the previous estimate.

4. *Tracking results*

Below an initial cloud density of 1e11 e/m^3, beam stability is maintained, but above that level, there is near exponential growth in both emittances and IP spot sizes, see Figure 5.1. A close-up of this blow-up is shown in Figure 5.2. This 'instability' is critical for future experiments in the BDS. Since cloud density relates to beam-cloud focusing, if the initial density is above the threshold, these focusing effects will be magnified.

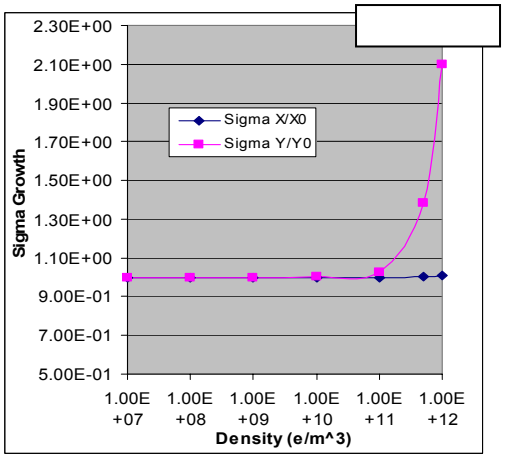

The beam emittance is constant with a cloud density of 1e10 e/m^3 for the entire length of the beam line, however the emittance increases greatly with a cloud density of 1e12 e–/m^3 near the end of the beam line. The same is true for spot sizes. This spot size increase appears to be dominated by the electron cloud close to the IP region.

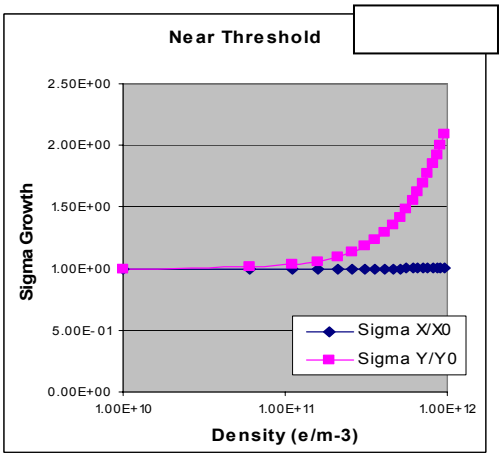

At this point, we tried to separate the relative importance of the nonlinear aberrations to the direct focusing effects. To see which was more important, we tracked a beam with zero energy spread through the lattice with the sextupoles on and sextupoles off. In both cases, we observed a similar threshold at an initial electron density of 1e11 e/m^3, indicating that the breakdown of the chromatic correction section is not the dominant contribution to the increase in the IP spot size.

Finally, we studied the impact of a more realistic energy spread in the beam. Figure 5.1 corresponds to the default uncorrelated rms energy spread of 3e–4 without a correlated contribution. We tried increasing the uncorrelated spread to 2e–3 and then tried adding a 'batman' energy distribution with a full width of 8e–3 representing the beam with an energy spread more similar to that from the linac. The tracking resulted in very similar thresholds in all these cases. However, the cases with the smallest energy spread had the largest increases in the spot sizes as shown in Figure 5.3.

FIGURE 5.3

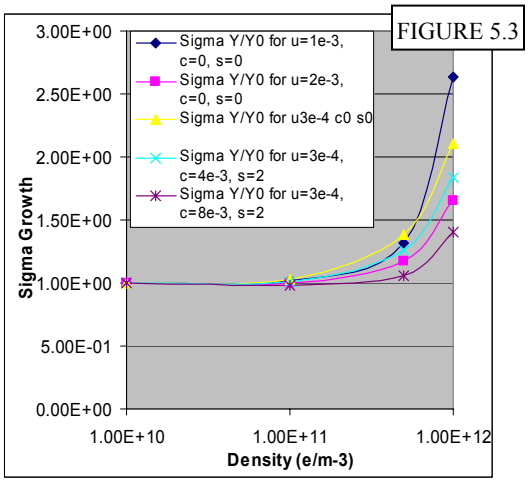

5. Positron Bunch and Electron Cloud Distributions

There is a significant increase in the spot size at the IP. To further understand the cause of this increase, it is useful to look at both the electron cloud density along the bunch and transverse beam size along the bunch. The initial electron cloud is uniformly distributed however, during the bunch passage, the electrons will be focused and the density at the center of the beam will increase. This density increase is a strong function of the electron bounce frequency in the positron beam. During much of the BDS where the beta functions and beam sizes are large, the electron bounce frequency is $<< 1/\sigma_z$ and the electron cloud slowly increases in density along the bunch length.

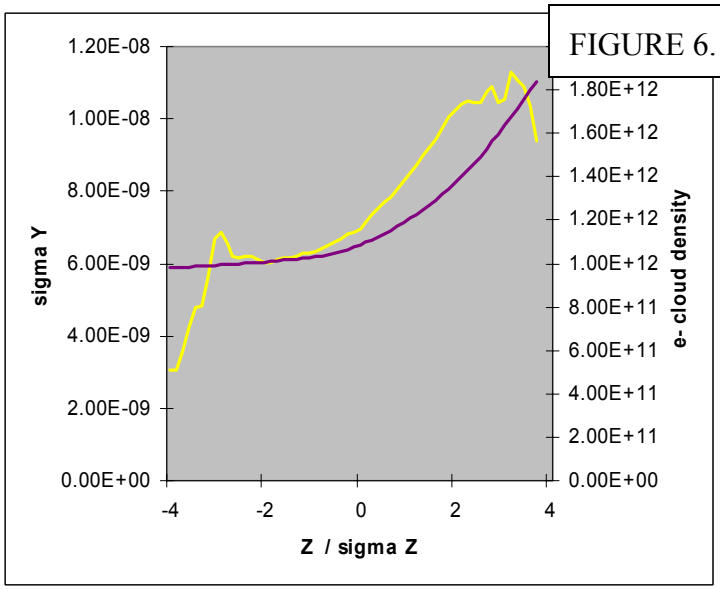

FIGURE 6.1

In Figure 6.1, both the vertical rms size of the positron beam and electron cloud density is plotted as a function of the longitudinal position in the positron beam for a case with an electron cloud density of 1e12 e/m^3. This is the "integrated" vertical beam size increase at the IP while the electron density is plotted at a location about 100 meters upstream of the IP where β_x and β_y are both roughly 30 km which is typical of the regions that contribute most to both the change in the phase advance and the change in the IP waist. There are few particles in the tails of the beams and thus the beam size is dominated by numerical noise but over the core region (from +/– 2 σ_z) the increase in the beam size resembles the increase in the electron density as one might expect.

6. Summary

Electron cloud instability can severely disrupt the normal passage of a positron beam through the beam delivery system of a normal conducting linear collider. The existence of a threshold density in the BDS at a density of roughly 1e11 e/m^3 suggests one solution: reducing cloud density to lower levels to minimize beam blow-up. It should be noted that these studies have been performed assuming a 250 GeV beam and the effects will at least scale as $1/\sqrt{\gamma}$ and most likely $1/\gamma$. Thus, these electron cloud effects will be very important for operation at the Z-pole where the threshold density will be five times lower.

This study has assumed an initial electron cloud that does not depend on location along the BDS beam line. Because of the different chamber geometries, the different levels of synchrotron radiation, and the different magnetic fields, different electron cloud densities will exist at different parts of the beam line and this should be included in future studies. Furthermore, this study assumed a single bunch and an initial electron cloud that is uniform spatially. Future studies should treat multiple bunches and the electron cloud generation through the BDS.

7. References

1. P. Emma, T. Raubenheimer, F. Zimmermann, "Emittance dilution by ions in the SLC Arcs," 4th European Particle Accelerator Conference, London, England (1994).
2. D. Bates, "Tutorial on CLOUD MAD," SLAC (2003).
3. M. Sands, *The Physics of Electron Storage Rings: An Introduction*, UC Santa Cruz (1970).